CENTER FOR TRANSPORTATION INFRASTRUCTURE AND SAFETY

MISSOURI S&T

Mechanical Characteristics of Low-cost Hybrid Fiber Reinforced Polymer

by

Mohamed ElGawady

NUTC R343

A National University Transportation Center at Missouri University of Science and Technology

Disclaimer

The contents of this report reflect the views of the author(s), who are responsible for the facts and the accuracy of information presented herein. This document is disseminated under the sponsorship of the Department of Transportation, University Transportation Centers Program and the Center for Transportation Infrastructure and Safety NUTC program at the Missouri University of Science and Technology, in the interest of information exchange. The U.S. Government and Center for Transportation Infrastructure and Safety assumes no liability for the contents or use thereof.

Technical Report Documentation Page

1. Report No. NUTC R343	2. Government Accession No.	3. Recipient's Catalog No.
4. Title and Subtitle Mechanical Characteristics of Low-Cost Hybrid Fiber Reinforced Polymer	5. Report Date July 2014	
	6. Performing Organization Code	
7. Author/s Mohamed ElGawady	8. Performing Organization Report No. Project # 00042525	
9. Performing Organization Name and Address Center for Transportation Infrastructure and Safety/NUTC program Missouri University of Science and Technology 220 Engineering Research Lab Rolla, MO 65409	10. Work Unit No. (TRAIS)	
	11. Contract or Grant No. DTRT06-G-0014	
12. Sponsoring Organization Name and Address U.S. Department of Transportation Research and Innovative Technology Administration 1200 New Jersey Avenue, SE Washington, DC 20590	13. Type of Report and Period Covered Final	
	14. Sponsoring Agency Code	

15. Supplementary Notes

16. Abstract

This report deals with the experimental investigation of using large deformable FRP, $\pm 45°$ oriented fibers, in concrete-filled fiber tubes (CFFT) under axial cyclic compressive loading. In addition, this report presents finite element modeling (FE) of CFFTs with large rupture strain FRP (LRS-FRP). The LRS-FRP is made with polyethylene naphthalate (PEN) and polyethylene terephthalate (PET) fibers. The PEN and PET fibers are environmentally friendly as they are made from recycled materials (e.g. bottles). They have high ultimate strain ($> 5.0\%$) however their elastic modulus is low. The experimental work consists of two CFFT cylinders have outer three layered FRP tube with fiber oriented at $\pm 45°$ and one CFFT cylinder has three hybrid-layered FRP [$\pm 45/0$]. The investigated cylinders are tested under axial cyclic compressive loading. The FE study investigates six cylinders of PET-FRP and three cylinders of PEN-FRP. One, two and three layers of each type are investigated in this study. The FE investigated cylinders are numerically analyzed under axial monotonic compressive loading using LS-DYNA. The experimental results presented in this report indicate that the angle-ply fibers have ability to dissipate high energy and achieve good ductility. The angle-ply fibers are reorienting during loading before reaching the rupture strain without considerable enhancement in the compressive strength. The FE results showed that the thick LRS-FRP achieved much better behavior in strength and ductility than the conventional FRP (glass and carbon). This indicated that the FRP ultimate strain had a great effect on the concrete confinement even if the elastic modulus was low.

17. Key Words Seismic behavior, FRP	18. Distribution Statement No restrictions. This document is available to the public through the National Technical Information Service, Springfield, Virginia 22161.		
19. Security Classification (of this report) unclassified	20. Security Classification (of this page) unclassified	21. No. Of Pages 23	22. Price

Form DOT F 1700.7 (8-72)

Mechanical Characteristics of Low-Cost Hybrid Fiber Reinforced Polymer

ABSTRACT

This report deals with the experimental investigation of using large deformable FRP, ± 45° oriented fibers, in concrete-filled fiber tubes (CFFT) under axial cyclic compressive loading. In addition, this report presents finite element modeling (FE) of CFFTs with large rupture strain FRP (LRS-FRP). The LRS-FRP is made with polyethylene naphthalate (PEN) and polyethylene terephthalate (PET) fibers. The PEN and PET fibers are environmentally friendly as they are made from recycled materials (e.g. bottles). They have high ultimate strain (> 5.0%) however their elastic modulus is low. The experimental work consists of two CFFT cylinders have outer three layered FRP tube with fiber oriented at ± 45° and one CFFT cylinder has three hybrid-layered FRP [± 45/0]. The investigated cylinders are tested under axial cyclic compressive loading. The FE study investigates six cylinders of PET-FRP and three cylinders of PEN-FRP. One, two and three layers of each type are investigated in this study. The FE investigated cylinders are numerically analyzed under axial monotonic compressive loading using LS-DYNA. The experimental results presented in this report indicate that the angle-ply fibers have ability to dissipate high energy and achieve good ductility. The angle-ply fibers are reorienting during loading before reaching the rupture strain without considerable enhancement in the compressive strength. The FE results showed that the thick LRS-FRP achieved much better behavior in strength and ductility than the conventional FRP (glass and carbon). This indicated

that the FRP ultimate strain had a great effect on the concrete confinement even if the elastic modulus was low.

INTRODUCTION

The use of fiber-reinforced polymer (FRP) has grown rapidly in the past two decades. The main purpose of using FRP is to enhance the strength and ductility of a structural member. FRP fibers confine the concrete structural element and in turn increase its compressive strength. The increased compressive strength is known as the confined compressive strength. The increase of strength happens only after the concrete core begins to dilate. Hence, FRP fibers act to the concrete core by a passive confinement achieving higher strength. FRP tubes have gained acceptance as an alternative to steel tubes in concrete filled steel tubes (CFST). CFFTs have many advantages such as light weight-to-strength ratio, high confinement and corrosion resistance compared to steel tubes. Seismic behavior of CFFT columns has been studied ((e.g. Shin and Andrawes 2010, Zhu et al. 2006). Dawood et al. (2012) and ElGawady and Sha'lan (2011), ElGawady et al. (2010)).

Au and Buyukozturk 2005 investigated the effect of fiber orientation on the confinement in CFFT cylinders. It was concluded that the angular fiber jackets showed a ductile failure modes with fiber reorientation mechanism. By this mechanism the fiber reoriented during loading which dissipating a high energy before reaching fiber rupture without considerable strength enhancement.

The most common FRP composites are made with carbon (CFRP), glass (GFRP) and aramid (AFRP). Such composites have linear elastic stress-strain relations with a rupture failure strain ranged around 1.5% to 3.0%. Recently, new FRP composites have been introduced as

alternatives to the common FRP (CFRP, GFRP and AFRP). These composites are made of polyethylene terephthalate (PET) and polyethylene naphthalate (PEN) fibers. However such composites have low elastic modulus, they have large rupture strains (LRS) usually larger than 5.0%. PET-FRP and PEN-FRP are usually made from recycled bottles. Therefore they are much cheaper than the conventional FRP. Recently, some experimental works have been conducted to investigate the performance of LRS FRP for jacketing RC columns (Anggawidjaja et al. 2006; Dai and Ueda 2012). These researches have shown that the columns reached the ultimate state without FRP rupture.

This report is primarily concerned with the behavior of the CFFT columns wrapped with large deformable FRP under axial compressive loading and their finite element modeling (FE). The report begins with the experimental work investigating the FRP jacketing of CFFT using the angle-ply fibers (± 45°) and hybrid FRP (± 45°/0). Then the FE study concentrates on the modeling CFFT confined with LRS-FRP. Verification of the FE model will be conducted with the experimental work.

EXPERIMENTAL PROGRAM

Test Specimens

Three concrete-filled fiber tubes (CFFT) specimens were investigated during the course of this research (Table 1) prepared and tested. Two CFFT cylinders (CFFT-1 & CFFT-2) had outer three layered FRP tube with fiber oriented at ± 45°. CFFT-1 cylinder was prepared using carbon fiber (CFRP) and CFFT-2 cylinder was prepared using glass fiber (GFRP). However, CFFT-3 cylinder had three hybrid-layered FRP tube. The first two layers of CFFT-3 were prepared with

glass fiber (GFRP) oriented at ± 45° and the outer layer was prepared with unidirectional glass fiber (GFRP). All specimens were tested under axial cyclic compressive loading.

The specimens had an outer diameter of 8.25 inch and a height of 16 inch. The FRP tubes of CFFT-1 and CFFT-2 were prepared manually by a wet-layup process on sonotube and were used as a mold for concrete pouring. The last wrapped layer of FRP tube was provided with 30% overlap to prevent premature debonding failure. The first two layers of the FRP tube of CFFT-3 were prepared manually by a wet-layup process on sonotube and were used as a mold for concrete pouring. However the outer third layer was wrapped on the two ± 45° layers after 56 days of concrete pouring.

The studied parameters were the effect of fiber orientation on the overall strength and ductility of CFFT cylinders. Table 1 shows the specimens details.

Table 1: Specimens descriptions

Specimen number	FRP tube	Outer diameter (in)	Concrete cylindrical strength f_c' (psi)
CFFT-1	CFRP- Three ± 45° layers		
CFFT-2	GFRP- Three ± 45° layers	8.25	8,000
CFFT-3	GFRP- Two ± 45° layers + one 0° layer		

Material Properties

Table 2 shows the mix design of the used SCC. The average cylindrical concrete compressive strength (f_c') at 56 days is 8,000 psi for five standard cylinders 6" x 12". One of these cylinders was tested under cyclic loading as explained later in this report and the others were tested under monotonic loading with a displacement rate of 0.02 in/min.

Table 2: SCC mixture proportions

w/cm	Cement (lb/cy)	Fly Ash (lb/cy)	Water (lb/cy)	Fine aggregate (lb/cy)	Coarse aggregate (lb/cy)	HRWRA (lb/cy)	VEA (lb/cy)
0.38	590	295	336	1411	1411	3.6	1.2

According to ASTM D3039, longitudinal and radial coupons were cut from the one layer GFRP tubes of orientation at $\pm 45°$. One horizontal and one vertical strain gauge were attached to the mid height of the longitudinal FRP coupon as shown in figure 1 (a). Two strain gauges were attached to the mid of the radial disk as shown in figure 1 (b). Under tensile tests with a displacement loading rate of 0.05 in/min, all FRP coupons whether longitudinal or radial failed by debonding between the two 45° plies [$+45^o$ and -45°] without fiber rupture as shown in figure 1. The ultimate stress was 10,500 psi (Figure 2). The saturated FRP with fiber orientation at 45° has a structure depends on fibers in two perpendicular directions [$+45^o$ and -45°] and adhesive material between them. Therefore this type of laminates works globally. As a result, the fibers did not work in the coupon tests as the width of the strip is only 1 inch so there is no fibers continuity.

The properties of the FRP here were referenced based on the manufacturer data sheet of Tyfo® BCC and Tyfo® BC of FRP tubes oriented at $\pm 45°$ and Tyfo® SHE-51 of unidirectional FRP tube. The manufacturer tensile strength, Young's modulus and maximum elongation of GFRP laminate oriented at $\pm 45°$ based on a nominal thickness of 0.034 inch are 40,500 psi,

2,700 ksi and 1.50 % respectively. The manufacturer tensile strength, Young's modulus and maximum elongation of CFRP laminate oriented at ± 45° based on a nominal thickness of 0.034 inch are 95,850 psi, 6950 ksi and 1.40 % respectively. The manufacturer tensile strength, Young's modulus and maximum elongation of unidirectional GFRP laminate based on a nominal thickness of 0.05 inch are 83,400 psi, 3,790 ksi and 2.20 % respectively. The properties of FRP tubes are summarized in table 3.

Table 3: Properties of saturated FRP according to manufacturer's data

Material	Nominal thickness/layer (in)	Young's modulus, E (ksi)	Tensile strength (psi)	Ultimate strain (%)
CFRP ± 45°	0.034	6,950	95,850	1.40
GFRP ± 45°	0.034	2,700	40,500	1.50
GFRP- unidirectional	0.05	3,790	83,400	2.20

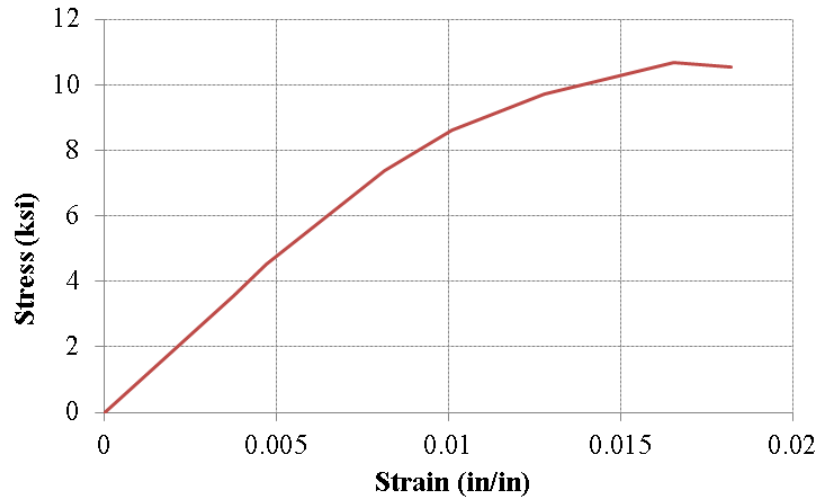(a)   (b)

Figure 1: (a) Longitudinal FRP coupon; (b) Radial FRP coupon

Figure 2: Strain-stress curve for FRP radial coupon

Experimental Set-up and Instrumentation

Compression tests were carried out using MTS machine with a loading rate of 0.02 in/min. All test data, including the strains, loads, and displacements, were recorded simultaneously using a data acquisition system. Two horizontal and two vertical strain gauges were installed on the outer surface at the mid-height of the FRP tube. In addition, two string potentiometers were attached on the outer surface of the FRP tube to obtain the axial deformation of the middle region of 5.5 in for each specimen.

Loading Schemes

All specimens were tested under compression loading on cyclic scheme as shown in figure 3. The cyclic compression involved full loading/unloading cycles, where the unloading of each cycle was designed to terminate at a 100 lb (near zero) and the reloading of each cycle was designed to terminate at the unloading displacement of the same cycle. The loading scheme

followed nine steps started at axial strain of 0.125 % and was increased gradually until failure of the specimen. Each loading step repeated three cycles.
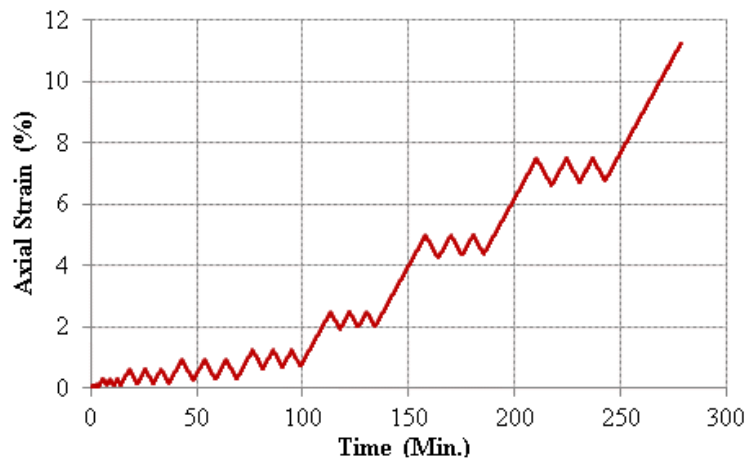
Figure 3: Cyclic loading scheme

EXPERIMENTAL RESULTS AND DISCUSSIONS OF COMPRESSION TESTS

The envelope axial strain-load curves of the cyclic curves of all specimens are shown in figure 4. All specimens had almost the same initial stiffness up to load level of 410 kips at ultimate axial strain of 12.0%. It was worthy noted that the cylinders with FRP tubes oriented at $\pm 45°$ (CFFT-1 and CFFT-2) had only one slope up to the ultimate load. The reason for that was the effect of the 45° FRP. The angle-ply FRP has an ability to give high ductility by the reorientation phenomenon (Au and Buyukozturk 2005). Under axial loading, the angular fiber reoriented from the initial case (+45/-45) toward the hoop direction. Therefore, CFFT-1 cylinder reached to the ultimate load of 413 kips without fiber rupture. It can be noted also in figure 4 that the load started to increase after axial strain of 6.0% in CFFT-1 which means the fibers were reoriented to close to the hoop direction. However, CFFT-2 cylinder achieved higher axial capacity of 443 kips, it was ruptured earlier than CFFT-1 at axial strain of 4.0%. It can be concluded that the GFRP was reorienting faster than the CFRP hence the fibers were much

closer to the hoop direction after the reorientation. That explained also why CFFT-2 achieved

higher capacity than CFFT-1.

CFFT-3 cylinder with hybrid FRP tube, fiber orientations were ± 45°/0, had a different

behavior than CFFT-1 and CFFT-2. It had two slopes before reaching the ultimate capacity of

457 kips. The strength dropped suddenly to 300 kips after reaching the ultimate axial capacity

because of rupture of some parts of unidirectional fibers. The strength was gradually decreased

up to full rupture of the FRP tubes at ultimate axial strain of 7.0%. It was clear in figure 4 that

CFFT-3 cylinder had better overall behavior in strength and ductility, appeared in the axial

strain, than CFFT-2. However CFFT-3 had higher strength than CFFT-1 cylinder, CFFT-1

cylinder had considerable higher ductility. Figure 5 shows the failure modes of the tested

cylinders. Table 4 summarizes the experimental results of the tested cylinders. The confined

concrete (f_{cc}') strengths and their ratio to the unconfined concrete strength (f_c') are summarized
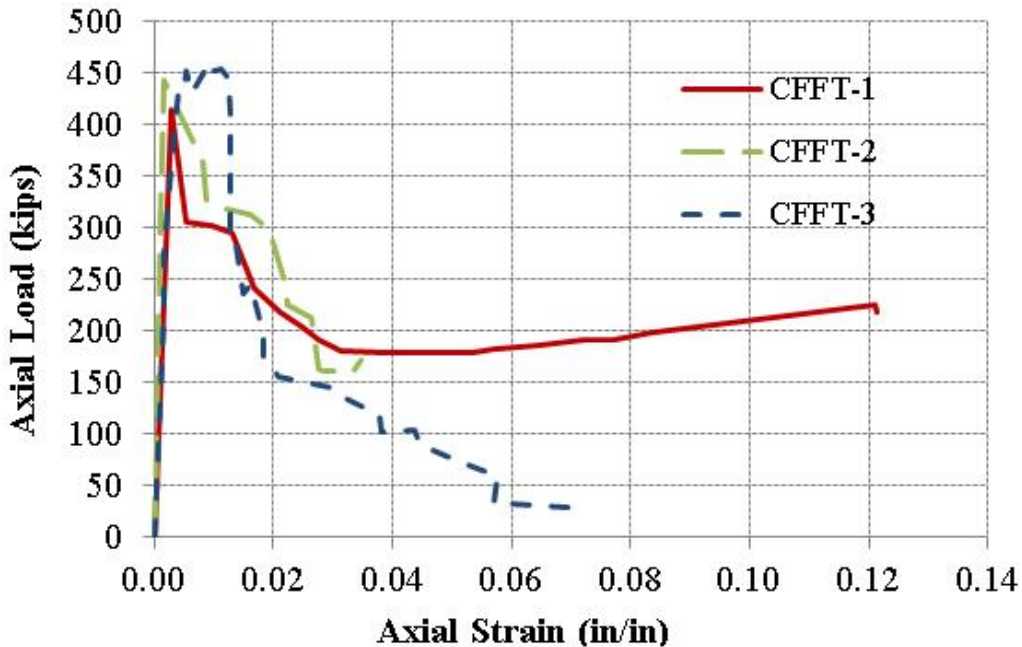
in Table 4.

Figure 4: Axial strain-load relations for tested cylinders

CFFT-1   **CFFT-2**   **CFFT-3**

Figure 5: Modes of failure of tested cylinders

Table 4: Experimental results of tested cylinders

Specimen number	Axial capacity (kips)	Ultimate axial strain	f'_{cc} (psi)	f'_{cc} / f'_c	FRP rupture
CFFT-1	413.0	12.0	7,726.0	0.97	No
CFFT-2	443.0	4.0	8,287.0	1.04	Yes
CFFT-3	457.0	7.0	8,549.0	1.07	Yes

FINITE ELMENT MODELING

The purpose of the FE study in this research is to investigate the performance of the new FRP category (PET and PEN) comparable to the conventional FRP (GFRP and CFRP). PET-600, PET-900 and PEN-600 were investigated in this study. The difference between the type of 600 and the type of 900 is only the sheet thickness. One, two and three layers were studied for

each type. The PET-600 and PEN-600 sheet thicknesses of one, two and three layers are 0.034 in, 0.067 in and 0.10 in, respectively. The PET-900 sheet thicknesses of one, two and three layers are 0.050 in, 0.10 in and 0.15 in, respectively. Table 5 summarizes the variables of the investigated cylinders.

Table 5: Summary of cylinders variables

Specimen number	FRP type	Total thickness (in)	No. of layers
PET-600-I		0.034	One
PET-600-II	PET-600	0.067	Two
PET-600-III		0.100	Three
PET-900-I		0.050	One
PET-900-II	PET-900	0.100	Two
PET-900-III		0.150	Three
PEN-600-I		0.034	One
PEN-600-II	PEN-600	0.067	Two
PEN-600-III		0.100	Three

Geometry

The cylinders under consideration in this study were investigated numerically under monotonic axial load with displacement control in LS-DYNA software. Each cylinder had a circular cross-section with an outer diameter of 8.25 in and a height of 16 in inserted between two rigid cubic steel plates with dimensions 9 in x 9 in x 2 in (Fig. 6). The concrete cylinder was modeled using solid elements. These elements had average dimensions of 0.36 in. x 0.60 in. x 0.50 in. The rigid steel plates were modeled by solid elements. These elements had dimensions of 0.50 in. x 0.50 in. x 0.50 in. The outer FRP tube was simulated using shell elements. A typical element dimension was 0.81 in. x 0.60 in. All solid elements were modeled with constant-stress and one-point quadrature to reduce the computational time. Hourglass control was used to avoid

spurious singular modes (i.e., hourglass modes) for solid elements. The hourglass value for all models was taken as the default value of 0.10.

Contact elements surface-to-surface were used to simulate the interface between the concrete cylinder and the outer FRP tube. Node-to-surface contact elements were used between the rigid plates and the cylinder (the concrete cylinder and the FRP tube).

(a) (b) (c) (d)
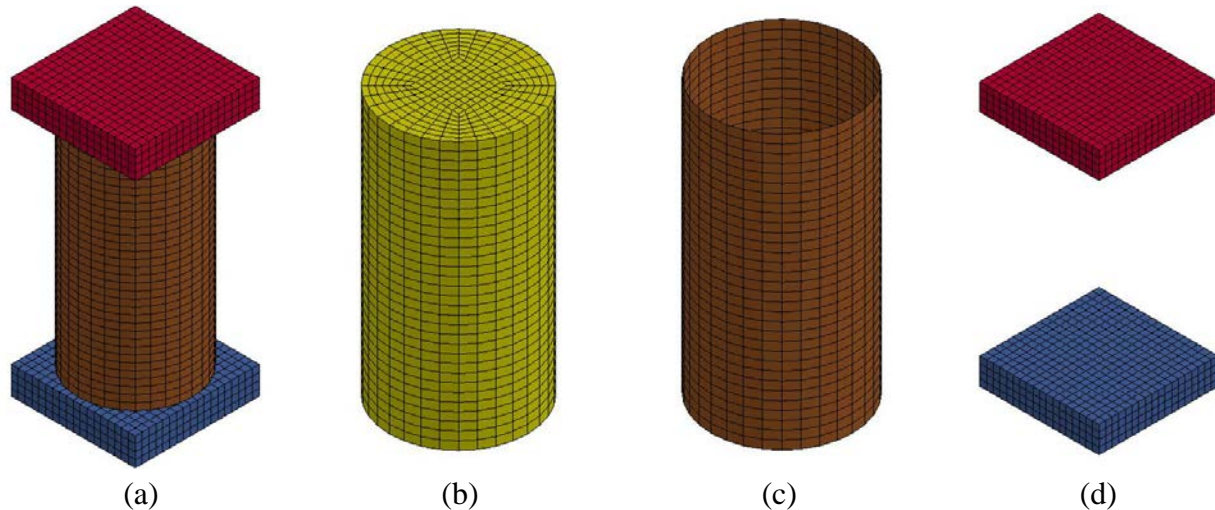
Figure 6: Finite element model components: (a) general view, (b) concrete cylinder, (c) FRP tube, (d) top and bottom rigid plates

Material models

Different material models are available in LS-DYNA to simulate concrete materials. Because the Karagozian and Case Concrete Damage Model Release 3 (K&C model) exhibited good agreement with the experimental results in collected previous studies, it was chosen for this study (Ryu et al. 2013). The model was developed based on the theory of plasticity. The model has three shear failure surfaces: yield, maximum, and residual (Malvar et al., 1997).

This material model has eighty parameters that can be either user defined or automatically generated. This report used the automatic generation option, with f_c' being the main input to the model. Another input to the model was the fractional dilation parameter (ω) which takes into consideration any volumetric change in concrete. In this report, the fractional dilation parameter

was taken as the default value of 0.50. The equation of state (EOS), which controls the compressive behavior of the concrete under triaxial stresses, was automatically generated, given f_c' and ω.

FRP tube

FRP material was modeled as an orthotropic material using "108-ortho_elastic_plastic" material. This model combines orthotropic elastic plastic behavior for shells only. This material is defined by the engineering constants: elastic modulus (E1), tangent modulus (E2), shear modulus (G), and poisson's ratio (PR), in the two principle axes (a and b). Additionally, the fiber orientation is defined by a vector. Failure criterion for FRP was defined using "000-add_erosion," by assigning the ultimate strain of FRP in "EFFEPS" card.

The material properties of PET-FRP and PEN-FRP composites have been studied by Dai et al. (2011). Such types of FRP have an approximately bilinear stress-strain relationships can be described in terms of two modulus of elasticity namely the initial elastic modulus (E1) and the tangent modulus (E2), tensile strength and rupture strain. The material properties of PET-FRP and PEN-FRP are summarized in Table 6.

Table 6: Material properties of new FRP category (reproduced after Dai et al. 2011 ©ASCE)

FRP Type	E1 (ksi)	E2 (ksi)	Tensile strength (ksi)	Rupture strain (%)
PET-FRP	2,595	1,203	109	8.71
PEN-FRP	3,915	1,740	111	6.26

Boundary conditions and loading

Displacements and rotations in all directions were prevented at the bottom of plate. Monotonic downward displacement loading was applied on the top plate for axial compressive loading until failure occurred. This failure was defined as the rupture of the FRP tube at either the ultimate strain or the crushing of the concrete cylinder.

Results and discussions

Model verification

In order to verify the FE model, numerical analysis was conducted for CFFT-3 cylinder and was compared to the experimental results. The axial strain was obtained by dividing the axial displacement by the cylinder height (12 in). The axial load applied on the cylinder was obtained from FE analysis by summation of the vertical reactions at the bottom plate. The axial strain versus the axial load from the experimental cyclic test and the FE monotonic numerical analysis are plotted in figure 7. The FE model, in general, was able to capture the behavior of the tested cylinder up to the maximum load. The initial stiffness in the FE was very close to the experimental up to a load level about 350.0 kips. The axial capacity of CFFT-3 were 457.0 kips and 460.0 kips during the experimental work and the FE analysis, respectively. The difference between the experimental strength and the FE strength was 0.66 %. The error is calculated as the absolute value of the difference between the experimental and the FE ultimate load divided by the experimental ultimate load. The ultimate axial strain of the tested cylinder was 0.07 and 0.017 during the experimental work and the FE analysis, respectively. The big difference between the ultimate axial strains experimentally and in the FE analysis was because the FE could not capture the reorientation of the angle-ply fibers (45°). However, this weakness of the FE model will not affect studying the LRS-FRP as they will be unidirectional fibers. The FE showed that the maximum FRP hoop strain at the mid height which matched the experimental

behavior as the first FRP rupture was at the mid height (Fig. 8(a)).FE results showed a very good

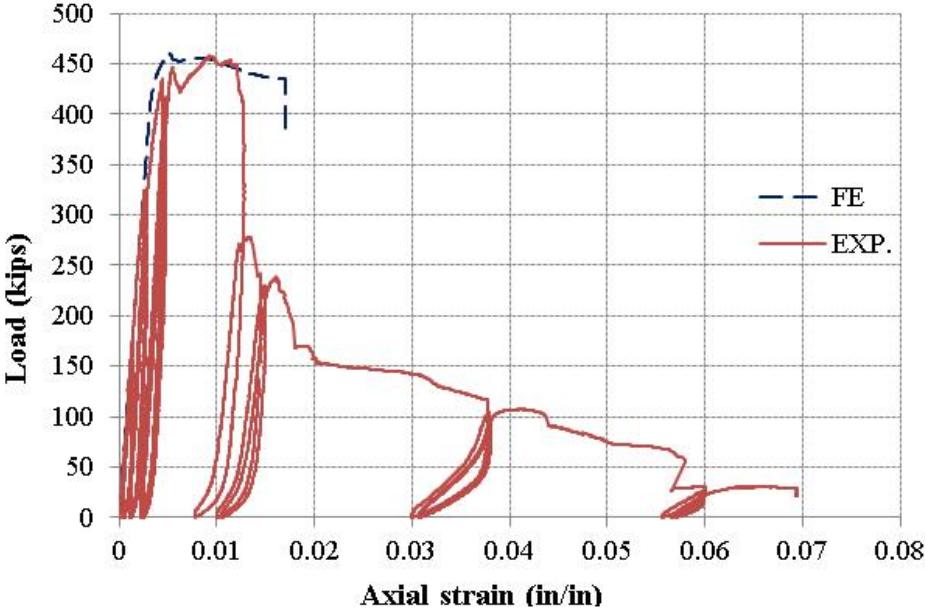agreement with mode of failure comparable to the experimental results (Fig. 8(b) & (c)).

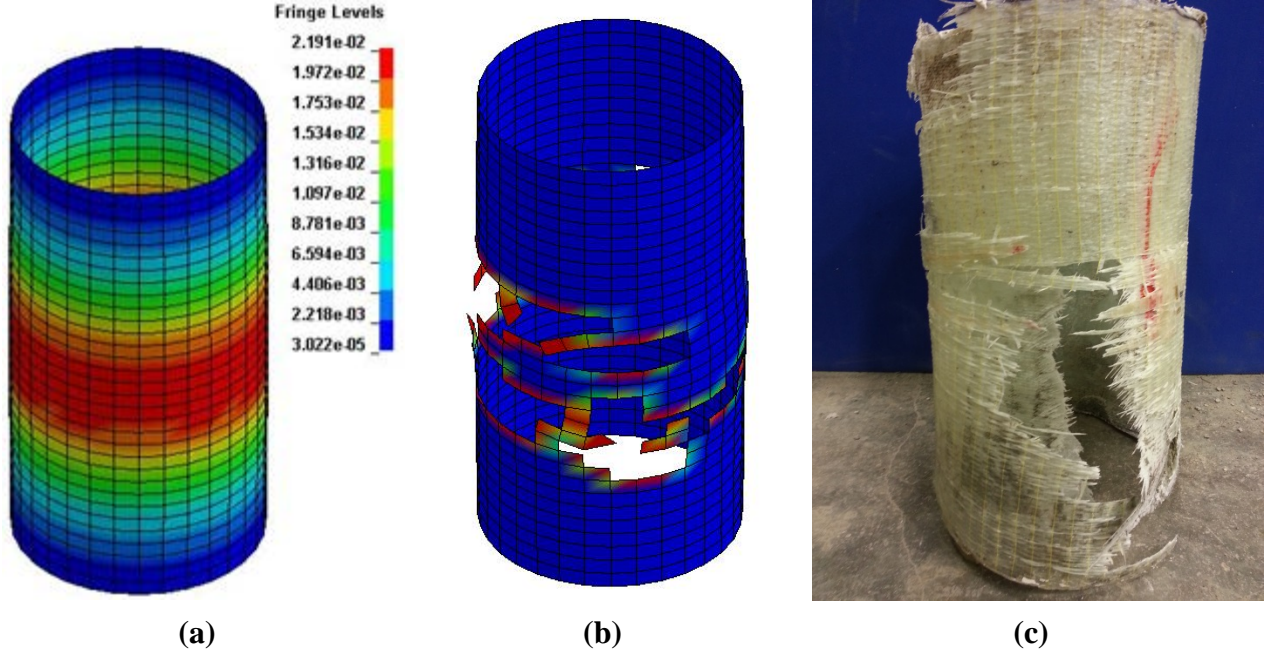**Figure 7: Experimental vs. FE axial strain-axial load curves of CFFT-3 cylinder**

(a)   **(b)**   **(c)**

Figure 8: (a) FRP hoop strains during FE, (b) FRP rupture during FE and (c) FRP rupture during experimental

All investigated cylinders, whether with PET or PEN fibers, were failed by FRP rupture. The ultimate axial capacity of PEN-I, II and III were 451.0 kips, 515.0 kips and 676.0 kips, respectively and with ultimate axial strains of 5.1%, 5.2% and 5.4%, respectively (Fig. 9). The ultimate axial capacity of PET600-I, II and III were 446.0 kips, 457.0 kips and 613.0 kips, respectively and with ultimate axial strains of 6.9%, 6.8% and 7.0%, respectively (Fig. 10). The ultimate axial capacity of PET900-I, II and III were 451.0 kips, 606.0 kips and 781.0 kips, respectively and with ultimate axial strains of 6.8%, 6.9% and 7.2%, respectively (Fig. 10). Table 7 summarizes the FE results. The confined concrete (f'_{cc}) strengths and their ratio to the unconfined concrete strength (f'_c) are summarized in Table 7.

Table 7: Summary of FE results

Specimen number	Ultimate axial load (kips)	Ultimate axial strain (%)	f'_{cc} (psi)	f'_{cc} / f'_c
PET-600-I	451.0	5.1	8,437.0	1.05
PET-600-II	515.0	5.2	9,634.0	1.20
PET-600-III	676.0	5.4	12,646.0	1.58
PET-900-I	446.0	6.9	8,343.0	1.04
PET-900-II	457.0	6.8	8,549.0	1.07
PET-900-III	613.0	7.0	11,467.0	1.43
PEN-600-I	451.0	6.8	8,437.0	1.05
PEN-600-II	606.0	6.9	11,336.0	1.42
PEN-600-III	781.0	7.2	14,610.0	1.83

It was clear that all investigated cylinders had the same initial stiffness as in this stage the behavior was controlled by the concrete only. It was worthy noted that the axial strain-axial load of PEN-600-III and PET-900-III had a bi-increasing relation, however all other cylinders behaved with increasing-decreasing relation. The strength of all cylinders except PEN-600-III

and PET-900-III returned to increase after decreasing. The reason for that was the effect of the friction force between the rigid plate and the concrete cylinders which made a considerable confinement at the top of the cylinder. This friction forces increased with increasing the axial displacement as the concrete dilation increased. It was noted from Figure 9 and 10 that PET-FRP gave a higher ductility than the PEN-FRP. A comparison between the experimental results of using fibers oriented at ± 45° and the finite element results of using LRS (600)-FRP of three layers (Fig. 11). It was noted that the higher strength could be achieved using PEN-FRP however the higher ductility could be achieved using CFRP oriented at ± 45°. It was also noted that CFFT-3, with hybrid fibers, and PET-600-III had the same axial strain but PET-600-III had around 34% higher strength. In general, it became clear that the cylinders with thick LRS-FRP achieved much better behavior than the conventional FRP. This indicated that the FRP ultimate strain had a great effect on the concrete confinement even if the elastic modulus was low.
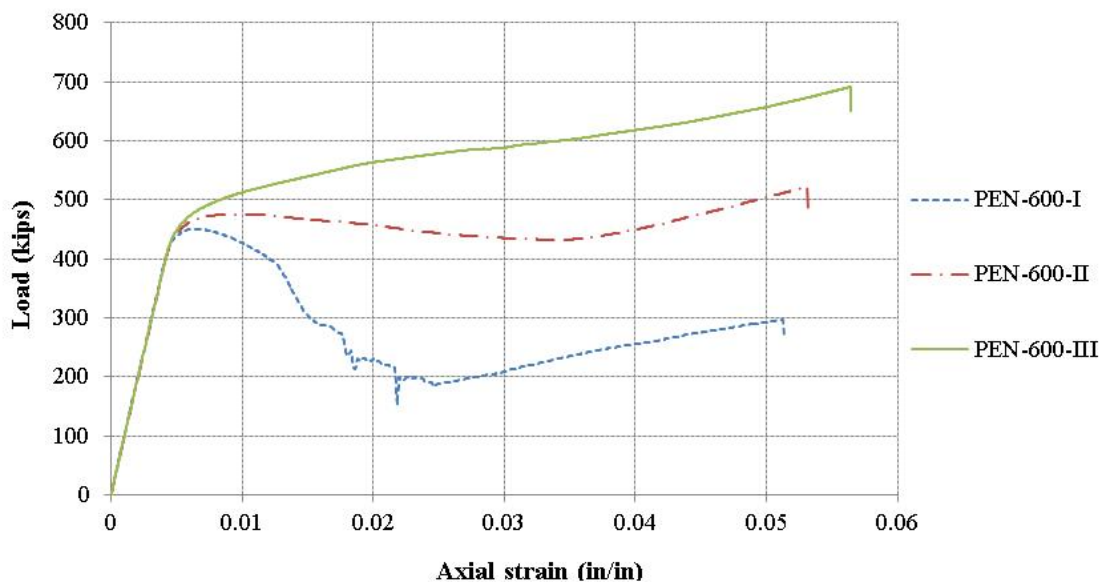
Figure 9: Axial strain-axial load of cylinders with PEN-FRP
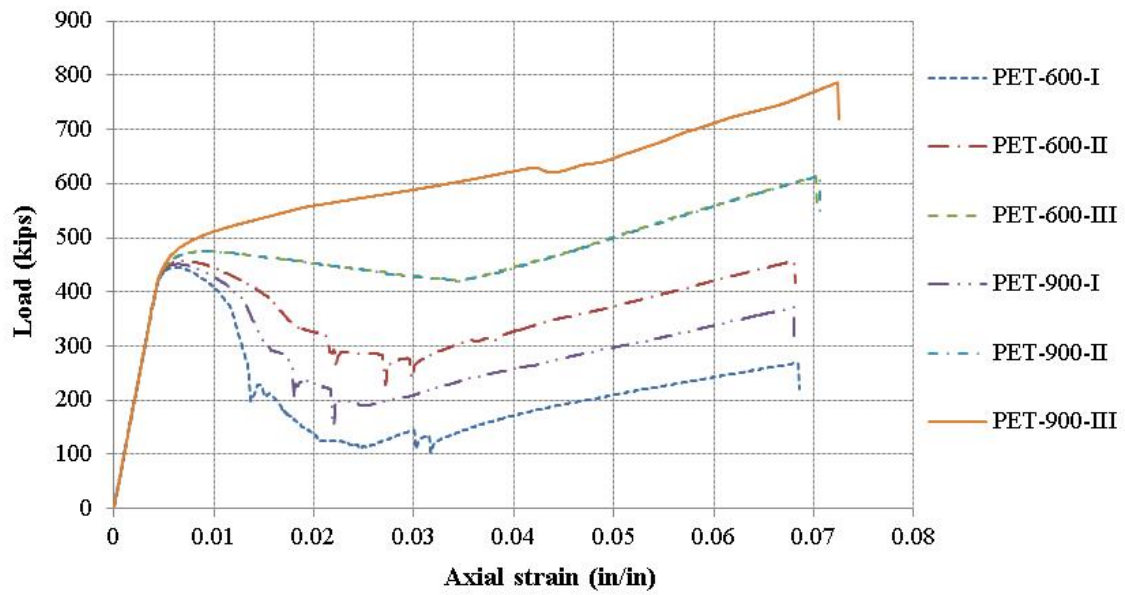
Figure 10: Axial strain-axial load of cylinders with PET-FRP
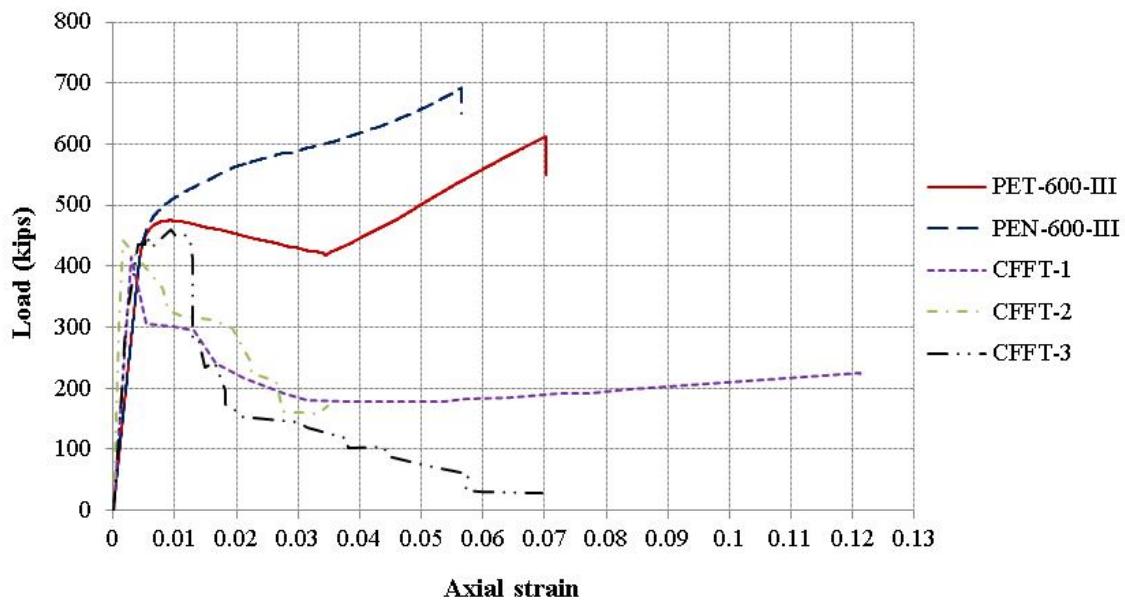
Figure 11: Axial strain-axial load of cylinders PET-600-III, PEN-600-III, CFFT-1, CFFT-2

and CFFT-3

CONCLUSIONS

This report has presented an experimental study of the use of large deformable FRP, ± 45° oriented fibers, in concrete-filled fiber tubes (CFFT) under axial cyclic compressive loading. Using large rupture strain (LRS) FRP in CFFTs under monotonic axial compressive loading has been examined in this study including PEN and PET FRP. It has been demonstrated that the cylinders confined by angle-ply fibers have an ability to dissipate energy by the mechanism of fiber reorientation. However, the bad effect of this mechanism is the very low enhancement on the compressive strength. It can be concluded numerically that the cylinders confined with LRS-FRP in general has better performance in strength and ductility than the cylinders confined with conventional FRP (glass and carbon) especially if LRS-FRP was thick. The ultimate strain had a considerable effect on the concrete confinement.

REFERENCES

Anggawidjaja, D., Ueda, T., Dai, J., and Nakai, H. (2006). "Deformation capacity of RC piers wrapped by new fiber-reinforced polymer with large fracture strain." Cem. Concr. Compos., 28(10), 914–927.

ASTM Standard A1067, 2012, "Test Coupons for Steel Castings," ASTM International, West Conshohocken, PA, 2012, 10.1520/A1067_A1067M-12A.

ASTM Standard D3039, 2008, Standard Test Method for Tensile Properties of Polymer Matrix Composite Materials," ASTM International, West Conshohocken, PA, 2008, 10.1520/D3039_D3039M-08.

Au, C. and Buyukozturk, O. (2005). "Effect of Fiber Orientation and Ply Mix on Fiber Reinforced Polymer-Confined Concrete." J. Compos. Constr., 9(5), 397–407.

Dai, J. G., and Ueda, T. (2012). "Strength and deformability of concrete members wrapped with fibre-reinforced polymer composites with a large rupture strain." Chapter 14, Innovative materials and techniques in concrete construction: ACES workshop, M. N. Fardis, ed., Springer, New York, 225–241.

Dai, J., Bai, Y., and Teng, J. (2011). "Behavior and Modeling of Concrete Confined with FRP Composites of Large Deformability." J. Compos. Constr., 15(6), 963–973.

Dawood, H., ElGawady, M., and Hewes, J. (2012). "Behavior of Segmental Precast Post-Tensioned Bridge Piers under Lateral Loads", ASCE Journal of Bridge Engineering, Vol. 17, No. 5, pp. 735-746.

ElGawady, M. and Sha'lan, A. (2011). "Seismic Behavior of Self-Centering Precast Segmental Bridge Bents." J. Bridge Eng., 16(3), 328–339.

ElGawady, M., Booker, A., and Dawood, H. (2010). "Seismic Behavior of Posttensioned Concrete-Filled Fiber Tubes." J. Compos. Constr., 14(5), 616–628.

Shin, M. and Andrawes, B. (2010). "Experimental Investigation of Actively Confined Concrete Using ShapeMemory Alloys". J. Eng. Struct. 32:3, 656-664.

Zhu, Z., Ahmad, I., and Mirmiran, A. (2006). "Seismic performance ofconcrete-filled FRP tube columns for bridge substructure." J. Bridge Eng., 11(3), 359–370.